Published in final edited form as:
J Am Chem Soc. 1999 March 10; 121(9): 1986–1987.

Binding Energies of Hexahydrated Alkaline Earth Metal Ions, $M^{2+}(H_2O)_6$, M = Mg, Ca, Sr, Ba: Evidence of Isomeric Structures for Magnesium

Sandra E. Rodriguez-Cruz, **Rebecca A. Jockusch**, and **Evan R. Williams**
Department of Chemistry, University of California Berkeley, California 94720

One strategy that has commonly been used to gain a more detailed understanding of ion chemistry in bulk solution is to investigate the structure and energetics of solvated ions in the gas phase. While solvation of singly charged metal ions has been studied extensively during the last two decades,[1] significantly less information about doubly and triply charged metal ions is known. Solvated divalent metal ions can now be readily produced using electrospray ionization (ESI).[2–5] This has led to a significant interest in obtaining thermochemical information about these ions with both experiment[3–5] and theory.[6–8] Kebarle and co-workers measured the Gibbs free energies of hydration for water molecules located in the second solvation shell of a variety of divalent metal ions using equilibrium experiments.[3] More recently, Posey and co-workers combined ESI with laser photofragmentation mass spectrometry to study divalent transition metal–ligand complexes with methanol in the second solvation shell.[4] Binding energies of inner solvent shell water molecules around Ni^{2+} and Ca^{2+} ions have been determined from blackbody infrared radiative dissociation (BIRD) experiments.[5] Here, BIRD kinetics of the hexahydrated alkaline earth metal ions, Mg^{2+}, Ca^{2+}, Sr^{2+}, and Ba^{2+}, are presented. At low temperatures, binding energies obtained from these kinetic data are directly correlated with the radii of the metal ions ($Mg^{2+} > Ca^{2+} > Sr^{2+} > Ba^{2+}$). In contrast, the binding energies at higher temperatures follow the trend $Ca^{2+} > Mg^{2+} > Sr^{2+} > Ba^{2+}$. This is the first direct evidence for two distinct gas-phase structures for a hydrated divalent metal ion.

Experiments were performed using an external electrospray ionization source Fourier transform mass spectrometer that has been described previously.[9] Hydrated alkaline earth $M^{2+}(H_2O)_n$ ions were generated from ~10^{-4} M aqueous solutions of the metal chloride salts using nanoelectrospray. Ions are loaded into the cell for 5 s during which time N_2 gas (10^{-6} Torr) is introduced. Dissociation kinetics of the mass-selected ion are investigated at pressures $<10^{-8}$ Torr. At these pressures, ion activation occurs by absorption of blackbody photons emitted by the heated vacuum chamber walls.[9–11] Unimolecular dissociation rate constants in the zero-pressure limit are measured as a function of temperature (22–140 °C) from which Arrhenius activation parameters are obtained. Under these conditions, the ion population does not have a Boltzmann distribution of internal energies.[10] Measured Arrhenius preexponentials and activation energies are smaller than those measured in the rapid energy exchange (REX) limit. To determine the threshold dissociation energies, master equation modeling of the kinetic data is necessary.[12] The application of the master equation model to obtain threshold dissociation energies has been described in detail previously.[11] The reverse activation barriers for these dissociation reactions should be negligible. Thus, the threshold dissociation energy should be equal to the binding energy.

Correspondence to: Evan R. Williams.

For all metal ion hydrates, dissociation occurs exclusively by loss of one water molecule. The kinetics are first order at all temperatures. Figure 1 shows the Arrhenius plots for dissociation of $M^{2+}(H_2O)_6$ and $M^{2+}(H_2O)_7$. For the heptahydrated clusters, the dissociation rate constants follow the trend $Ba^{2+} > Sr^{2+} > Ca^{2+} > Mg^{2+}$. This trend is consistent with the expected reactivity based on the ionic radii of the metals (water molecules attached to larger metal ions are expected to be less strongly bound). For the hexahydrated ions, this same ordering of rate constants is observed at low temperatures. In striking contrast, the order is $Ba^{2+} > Sr^{2+} > Mg^{2+} > Ca^{2+}$ at higher temperatures; the slope of the Arrhenius plot for $Mg^{2+}(H_2O)_6$ changes around 80°C! BIRD rate constants for the pentahydrated species have the same trend as that observed for the hexahydrated species at high temperature ($Ba^{2+} > Sr^{2+} > Mg^{2+} > Ca^{2+}$).[13] Thus, these dissociation kinetics do not follow the trend expected based on ionic radii. The change in the slope of the Arrhenius plot for Mg^{2+}-$(H_2O)_6$ shows the presence of two distinct gas-phase structuresfor this ion. The first-order behavior (>80% precursor ion depletion) at all temperatures indicates the presence of one structure or several structures that interconvert.

The measured zero-pressure limit Arrhenius parameters and the binding energies (E_o) obtained from master equation modeling of the kinetic data are given in Table 1. The low-temperature E_o's consistently increase with decreasing cation size. At high temperatures, the binding energy of the sixth water molecule to Mg^{2+} (21.1 kcal/mol) is less than that at low temperatures (23.5 kcal/mol). It is also slightly less than that for the larger calcium cation (21.6 kcal/mol). For $Mg^{2+}(H_2O)_6$, anomalously large radiative rate constants were used in the modeling in order to fit the kinetic data at low temperature. The reason for this is not clear, but this suggests that the error in E_o at low temperature may be larger than reported. The unexpected ordering of binding energies at high temperature is consistent with ΔH values recently reported by Kebarle and co-workers from equilibrium experiments at 170–225°C.[3a] Recent density functional theory (DFT) calculations by Pavlov et al.[8] have been used to evaluate structures for hydrated divalent magnesium and calcium ions, $M^{2+}(H_2O)_m$-$(H_2O)_n$, where m and n correspond to the number of water molecules in the first and second shell, respectively. The successive water binding energies ($\Delta E_{binding}$) reported for these structures are also included in Table 1.

To further investigate this unexpected reactivity of $Mg^{2+}(H_2O)_6$, we also performed DFT calculations on all four hexahydrated divalent metals.[14] Three different types of structures were studied in which the six water molecules are either all in the first shell or distributed between the first and second solvation shells around the metals. By the use of the nomenclature of Pavlov et al., the structures investigated were $M^{2+}(H_2O)_6$, $M^{2+}(H_2O)_5(H_2O)$,[15] and $M^{2+}(H_2O)_4(H_2O)_2$. Calculations indicate that the order of stability is $M^{2+}(H_2O)_6 > M^{2+}(H_2O)_5(H_2O) > M^{2+}(H_2O)_4(H_2O)_2$ for all of the metals. The energy differences between each of the higher energy structures and the $M^{2+}(H_2O)_6$ conformation are reported in Table 2. Also included in the table are the values of Pavlov et al.[8] for magnesium and calcium. At this level of theory, all three hexahydrated Mg^{2+} structures have energies within 5 kcal/mol. Several similar energy structures for hexahydrated barium ions were also found. However, no evidence of multiple gas-phase hexahydrated barium structures was observed over the temperature range of these experiments

Although the experimental evidence for two distinct structures for $Mg^{2+}(H_2O)_6$ is clear, the exact nature of these isomers is not. One possibility is that the isomers have different number of water molecules in the first and second shell. The results of DFT calculations show that all three hexahydrated Mg^{2+} structures investigated have 0 K energies within 5 kcal/mol (Table 2). The entropies of $Mg^{2+}(H_2O)_5(H_2O)$ and $Mg^{2+}(H_2O)_4(H_2O)_2$ under standard conditions are higher than that of $Mg^{2+}(H_2O)_6$. The opposite is true for the Ca^{2+}, Sr^{2+}, and Ba^{2+} hexahydrates. The anomalous entropy for $Mg^{2+}(H_2O)_6$ is presumably due to the crowding of the six water molecules around the much smaller metal ion. This would suggest that the higher temperature structure corresponds to a two-shell structure. Another possible explanation is that

one of the isomers is a salt-bridge structure (Scheme 1). Such a salt-bridge structure was found to be stable at the semiempirical PM3 level of theory, but not with the density functional levels of theory applied. The proton-transfer process necessary for the formation of a salt-bridge is expected to occur more readily for hydrated Mg than for the larger metal hydrates.[3b]

In conclusion, evidence for two distinct isomeric structures of $Mg^{2+}(H_2O)_6$ is presented. This is the first experimental evidence for two isomeric structures of hydrated metal dications. Binding energies of water to $Mg^{2+}(H_2O)_7$ and $Mg^{2+}(H_2O)_6$ (low temperature) follow the expected trend in cation size. These values for $Mg^{2+}(H_2O)_6$ (high temperature) do not. Calculations suggest that the most stable structure for $M^{2+}(H_2O)_6$ is one in which all of the water molecules are in the inner shell. However, further experiments and higher level calculations are necessary to definitively elucidate these structures.

Acknowledgements

The authors thank Dr. Maria Pavlov (University of Stockholm) for providing the coordinates for $Mg^{2+}(H_2O)_n$ and Ca^{2+}-$(H_2O)_n$. We also acknowledge the financial support provided by the National Science Foundation (CHE-9726183) and the National Institutes of Health (IR29GM50336-01A2, and fellowship support for R.A.J.).

References

1. a Castleman AW Jr, Bowen KH Jr. J Phys Chem 1996;100:12911–12944.and references therein. b Keesee RG, Castleman AW Jr. J Phys Chem Ref Data 1986;15:1011–1071. c Dzidic I, Kebarle P. J Phys Chem 1970;74:1466–1474. d El-Shall MS, Schriver KE, Whetten RL, Meot-Ner (Mautner) M. J Phys Chem 1989;93:7969–7973. e Dalleska NF, Honma K, Sunderlin LS, Armentrout PB. J Am Chem Soc 1994;116:3519–3528. f Berg C, Achatz U, Beyer M, Joos S, Albert G, Schindler T, Niedner-Schatteburg G, Bondybey VE. Int J Mass Spectrom Ion Processes 1997;167/168:723–734.
2. Schmelzeisen-Redeker G, Bütfering L, Röllgen FW. Int J Mass Spectrom Ion Processes 1989;90:139–150.
3. a Peschke M, Blades AT, Kebarle P. J Phys Chem A 1998;102:9978–9985. b Blades AT, Jayaweera P, Ikonomou MG, Kebarle P. J Chem Phys 1990;92:5900–5906.
4. Spence TG, Burns TD, Guckenberger VGB, Posey LA. J Phys Chem A 1997;101:1081–1092.
5. Rodriguez-Cruz SE, Jockusch RA, Williams ER. J Am Chem Soc 1998;120:5842–5843. [PubMed: 16479268]
6. a Katz AK, Glusker JP, Beebe SA, Bock CW. J Am Chem Soc 1996;118:5752–5763. b Markham GD, Glusker JP, Bock CL, Trachtman M, Bock CW. J Phys Chem 1996;100:3488–3497.
7. Glendening ED, Feller D. J Phys Chem 1996;100:4790–4797.
8. Pavlov M, Siegbahn PEM, Sandström M. J Phys Chem A 1998;102:219–228.
9. Price WD, Schnier PD, Williams ER. Anal Chem 1996;68:859–866.
10. a Price WD, Schnier PD, Jockusch RA, Strittmatter EF, Williams ER. J Am Chem Soc 1996;118:10640–10644. [PubMed: 16467929] b Dunbar RC, McMahon TB, Tholmann D, Tonner DS, Salahub DR, Wei D. J Am Chem Soc 1995;117:12819–12825.
11. a Price WD, Schnier PD, Williams ER. J Phys Chem B 1997;101:664–673. [PubMed: 17235378] b Jockusch RA, Williams ER. J Phys Chem A 1998;102:4543–4550. [PubMed: 16604163]
12. For this modeling, vibrational frequencies and transition dipole moments for the Mg^{2+}, Ca^{2+}, and Sr^{2+} systems were obtained at the RHF/STO-3G level and at the B3LYP/LANL2DZ level for $Ba^{2+}(H_2O)_6$ Microcanonical radiative rate constants are calculated using these values and varied over a 9-fold range to account for errors in the calculated values. For Mg^{2+}-$(H_2O)_6$, a 16-fold range was required to fit the data at low temperature. Dissociation rate constants are obtained by using RRKM theory and adjusted to provide REX limit A-factors between 10^{14} and $10^{17.5}$ s^{-1} to take into account a range of transition state entropies.
13. Manuscript under preparation.
14. Relative energies for the hexahydrated metal ions were calculated using the hybrid density functional method B3LYP. Geometry optimizations were done using the double-ζ basis set LACVP**, which incorporates an effective core potential for Ca, Sr, and Ba (Hay, P. J.; Wadt, W. R. J. Chem. Phys.

1985, 82, 299–310) and uses 6-31G** for Mg, O, and H. Single-point energy calculations were done at the optimized geometries replacing the basis sets on Mg, O, and H with the larger 6-311G++(2d, 2p) basis set. RHF frequency analyses confirmed that each structure is an energy minimum. Zero-point vibrational energies were calculated by scaling the RHF frequencies by 0.91. All of the calculations were performed using Jaguar v. 3.0 software (Schrodinger Inc., Portland, OR, 1997).

15. Two different $M^{2+}(H_2O)_5(H_2O)$ structures were studied; one in which the water in the second shell is hydrogen-bonded to one water in the inner shell, the other in which the outer water is hydrogen-bonded to two inner-shell water molecules. The latter structure is 4–6 kcal/mol more stable for all four hexahydrated metals.

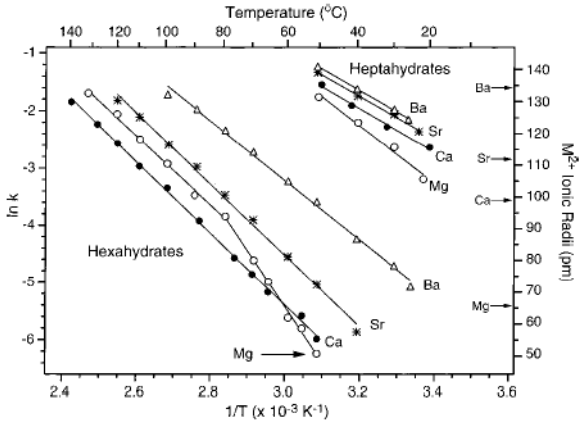

Figure 1.

Arrhenius plots obtained from blackbody infrared radiative dissociation data of the hexa- and heptahydrated alkaline earth metal ions; Mg^{2+} (○), Ca^{2+} (•), Sr^{2+} (*), and Ba^{2+} (▵).

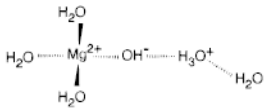

Scheme 1.

Table 1

Measured Zero-Pressure Limit Arrhenius Parameters and E_O Values Obtained from Master Equation Modeling for Loss of Water from $M^{2+}(H_2O)_6$ Ions[a]

M	E_a (kcal/mol)[b]	log A[b]	E_o (kcal/mol)[c]	$\Delta E_{binding}$ (kcal/mol)[d]
Mg	19.3 ± 0.6	10.3 ± 0.4	23.5 ± 1.6	24.5, 20.8,[ef] 19.6, 23.7[gh]
	12.3 ± 0.4	5.7 ± 0.2	21.1 ± 0.8	
Ca	12.4 ± 0.1	5.8 ± 0.1	21.6 ± 0.8	24.7,[e] 18.5,[f] 18.8,[g] 21.6[h]
Sr	12.4 ± 0.3	6.1 ± 0.2	20.6 ± 1.0	
Ba	10.3 ± 0.3	5.4 ± 0.2	17.9 ± 0.6	

[a] Previously reported B3LYP calculations of successive binding energies are also given.

[b] Reported errors are obtained from linear least squares analysis of the Arrhenius data.

[c] Reported errors indicate both experimental error as well as the range of parameters used in the modeling.

[d] Reference 8.

[e] $M^{2+}(H_2O)_6$.

[f] $M^{2+}(H_2O)_5(H_2O)$ where the water in the second shell is H-bonded to one water in the inner shell.

[g] $M^{2+}(H_2O)_5(H_2O)$ where the water in the second shell is H-bonded to two different waters in the first shell.

[h] $M^{2+}(H_2O)_4(H_2O)_2$.

Table 2

B3LYP Energy Differences between $M^{2+}(H_2O)_5(H_2O)$ and $M^{2+}(H_2O)_4(H_2O)_2$ and the Most Stable $M^{2+}(H_2O)_6$ Structure[a]

structure	ΔE(elec. + ZPE)[b] (kcal/mol)	ΔE_{total}[c] (kcal/mol)
$Mg^{2+}(H_2O)_5(H_2O)$[d]	2.3	4.9
$Mg^{2+}(H_2O)_4(H_2O)_2$	4.8	4.4
$Ca^{2+}(H_2O)_5(H_2O)$[d]	4.2	5.9
$Ca^{2+}(H_2O)_4(H_2O)_2$	9.6	8.7
$Sr^{2+}(H_2O)_5(H_2O)$[d]	3.2	
$Sr^{2+}(H_2O)_4(H_2O)_2$	7.5	
$Ba^{2+}(H_2O)_5(H_2O)$[d]	1.6	
$Ba^{2+}(H_2O)_4(H_2O)_2$	3.9	

[a] Previously reported values for Mg^{2+} and Ca^{2+} are also shown.

[b] This work;

[c] Values from Pavlov and co-workers (ref 8).

[d] Values reported for structures in which the second shell water molecule is hydrogen-bonded to two inner-shell water molecules.